Clinical Pharmacology
in Drug Development
2022, 11(6) 770–779

DOI: 10.1002/cpdd.1075

Assessment of Effects of Investigational TAK-931, an Oral Cell Division Cycle 7 Kinase Inhibitor on the QTc Intervals in Patients With Advanced Solid Tumors

Xiaofei Zhou[1], Paul Matthias Diderichsen[2], and Neeraj Gupta[1]

Abstract

TAK-931, a novel, selective, small-molecule inhibitor of cell division cycle 7 has been investigated in multiple clinical trials in patients with advanced solid tumors. An integrated analysis using data from 2 clinical studies assessed effects of TAK-931 on electrocardiogram QT intervals and heart rate (HR). Pharmacokinetic samples and matched triplicate electrocardiogram data were collected in 48 patients with cancer receiving oral administration of TAK-931 50 or 80 mg once daily. The relationships between TAK-931 plasma concentrations and the HR-corrected QT interval via Fridericia (QTcF) or population (QTcP) and HR were analyzed using linear mixed-effects models with fixed effects for day and time. At the geometric mean maximum TAK-931 plasma concentrations after administration of 50 mg, an HR change of 3.40 beats per minute (90%CI, 1.86-4.80) was predicted. Change in QTcF of −3.41 milliseconds (90%CI, −5.77 to −1.17) and QTcP of −2.02 milliseconds (90%CI, −4.15 to 0.0679) were estimated, indicating there was no effect of TAK-931 on the QT intervals at a recommended phase 2 dose of 50 mg once daily for 14 days in a 21-day cycle.

Keywords

cardiotoxicity, cell division cycle 7 inhibitor, concentration-QT, QTc interval, TAK-931

TAK-931, 2-[(2*S*)-1-azabicyclo[2.2.2]oct-2-yl]-6-(3-methyl-1*H*-pyrazol-4-yl)thieno[3,2-*d*]pyrimidin-4(3*H*)-one hemihydrate is a novel, selective inhibitor of cell division cycle 7 protein kinase with a time-dependent and adenosine 5′-triphosphosphate–competitive mechanism.[1–3] TAK-931 was selected as a next-generation, replication stress–inducing anticancer drug. It prolongs replication stress and stimulates follow-on mitotic aberrations.[2] TAK-931 also inhibits both in vitro and in vivo preclinical cancer models of proliferation, displaying a unique activity spectrum. TAK-931 has more antiproliferative activity against RAS-mutant cancer cell lines than those with wild-type alleles. Clinical studies have been investigating the safety, pharmacokinetics, and efficacy of TAK-931 in patients with advanced solid tumors.[4–6] Cytochrome P450 (CYP) 2D6 and CYP3A4/5 were the main CYP enzymes involved in the metabolism of TAK-931 based on in vitro CYP-mediated metabolism studies. Subsequent uridine diphosphate-glucuronosyltransferase (UGT)-mediated metabolism indicated that UGT1A9 was the primary UGT responsible for the metabolism of TAK-931. Although the potential for drug-drug interactions with strong CYP inhibitors was considered low, there was potential for drug-drug interaction with strong metabolic enzyme inducers such as rifampin. Therefore, strong metabolic enzyme inducers were prohibited in patients receiving TAK-931 treatment.[3] The population pharmacokinetic (PK) analysis using data

[1]Quantitative Clinical Pharmacology, Takeda Development Center Americas, Inc., Cambridge, Massachusetts, USA
[2]Certara USA, Inc., Princeton, New Jersey, USA

Submitted for publication 19 October 2021; accepted 27 December 2021.

Corresponding Author:
Neeraj Gupta, PhD, Quantitative Clinical Pharmacology, Takeda Development Center Americas, Inc., 40 Landsdowne Street, Cambridge, MA 02139
(e-mail: neeraj.gupta@takeda.com)

Fellows of the American College of Clinical Pharmacology: Neeraj Gupta, PhD.

from ≈200 patients with cancer who were treated with TAK-931 in the phase 1 and 2 clinical trials indicated that age (36-88 years), body weight (30-127 kg), Eastern Cooperative Oncology Group performance score, sex, race, mild or moderate renal impairment, and mild hepatic impairment had no clinically meaningful impact on TAK-931 apparent oral clearance, supporting the same starting dose of TAK-931 regardless of these patient-specific factors.[3] Hepatic metabolism was expected to be a major clearance pathway for TAK-931. Renal clearance accounted for only ≈8% of TAK-931 oral clearance, indicating that renal clearance plays a minor role in the elimination of TAK-931. This was consistent with the finding that creatinine clearance (≥30 mL/min) did not have a clinically meaningful impact on TAK-931 exposures based on the population PK analysis.[3]

Comprehensive assessment of QT prolongation potential is an important consideration in drug development. The International Council for Harmonization E14 guidelines have evolved to streamline drug development and improve regulatory decision making and product labeling for cardiac risks of new drugs.[7–9] There are various strategies to evaluate the QT prolongation potential for anticancer agents ranging from an integrated in vitro data assessment or conducting a dedicated evaluation study.[10–12] The current analysis used TAK-931 plasma concentrations and time-matched, centrally read, triplicate ECG data from 2 clinical studies (NCT03261947[5] and NCT03708211[6]) in which patients with advanced solid tumors received TAK-931 treatment to assess the effect of TAK-931 on corrected QT (QTc) intervals at clinically relevant doses.

Methods

Overview of Data

For this population model-based, concentration-QTc analysis, data were obtained for adult patients (aged ≥18 years) with advanced solid tumors who had participated in 2 clinical trials of TAK-931 (NCT03708211 and NCT03261947), as summarized in Table S1. All patients provided written informed consent. The study protocols were approved by review boards at each center, and the clinical trials were conducted in accordance with applicable regulatory standards and the International Conference on Harmonization Guideline for Good Clinical Practice.[13] TAK-931 was administered to patients on an empty stomach except water from 2 hours before taking the study drug until completion of collection of the 4-hour electrocardiogram (ECG)/PK postdose samples on days 1 and 3 to minimize the influence of food on ECGs.[14] Blood samples for measuring plasma TAK-931 concentrations were collected at times corresponding to ECG assessments, with resting ECG measurements collected immediately prior to blood sampling. The triplicate ECG were centrally read and averaged before the model-based analysis.

Analytical Methods

Plasma samples with dipotassium-ethylenediaminetetraacetic acid anticoagulant were analyzed for TAK-931 concentrations by a Good Laboratory Practice–validated turbo ion spray liquid chromatography–tandem mass spectrometry method. TAK-931-d_7 ($C_{17}H_{12}D_7N_5OS$) was used as the internal standard. Plasma samples were extracted by protein precipitation followed by high-performance liquid chromatography separation using a Phenomenex Luna Omega 1.6 μm Polar C18 column (2.1 × 50 mm; Phenomenex, Torrance, California) and mobile phases consisting of 1000:1 water/formic acid and 500:500:1 acetonitrile/methanol/formic acid. Mass spectrometer instrument settings were: API 5000/Analyst version 1.6.2 (SCIEX, Redwood City, California), ionization source/ionization mode of turbo ion spray/positive, and utilized selected reaction monitoring. The lower limit of quantification was 0.5 ng/mL. Within-day and between-day accuracy was between 0.0% and 94% and 0.5% and 6.0%, respectively. Within-day and between-day precision was ≤10.9% and ≤7.5%, respectively.

Software and Estimation Method

Assembly of the population concentration-ECG analysis data set used SAS® version 9.4 (SAS Institute, Cary, North Carolina). Nonlinear mixed-effects modeling software (NONMEM® version 7.3.0; ICON, Hanover, Maryland) was used for modeling. All model development and final analyses were based on the first-order conditional estimation method of NONMEM without interaction (FOCE). NONMEM was run through Pirana (Certara, Princeton, New Jersey) or Perl Speaks NONMEM (PsN version 4.8; Department of Pharmacy, Uppsala University, Uppsala, Sweden). R version 3.6.1 (R Foundation for Statistical Computing, Vienna, Austria) was used for the analysis of the analysis data set, statistical summaries, and modeling results. R was also used for model-based simulations.

Covariate Variables

Covariates evaluated in the models of Fridericia-corrected QT (QTcF) intervals, population-corrected QT (QTcP) intervals, and heart rate (HR) included continuous variables (baseline age, weight, and body mass index [BMI]) and categorical variables (sex [male or female], Eastern Cooperative Oncology Group status [ECOG], and study). Baseline covariates were obtained from observations on the first day of dosing or at participant screening. Missing continuous participant covariates were imputed by the median value of the study population during covariate model construction.

Missing categorical covariates were grouped with the most common covariate category during covariate model building.

Concentration—ECG Model Development

As a first step in the analysis, the appropriateness of the Fridericia and the population correction of observed QT intervals was evaluated by deriving the slope of uncorrected and corrected QT intervals vs corresponding RR intervals.

The ECG data were analyzed with a linear mixed-effects modeling approach. Plasma concentrations of TAK-931 were evaluated as predictors of QTcF, QTcP, and HR in separate models.

The concentration-QTcF analysis was considered the primary analysis and was based on a model with a random intercept, linear relationship with no delay in the effect of TAK-931 upon QTcF. The analysis used the following equation for QTcF:

$$QTcF = BQTcF + \eta_{BQTcF} + COVTIME_i + SLP \cdot C_{TAK931} + \varepsilon_{QTcF} \quad (1)$$

where $BQTcF$ is the typical baseline QTcF interval before dose administration; η_{BQTcF} is interindividual random effects associated with baseline QTcF; $COVTIME_i$ is an unstructured correction of time effect (study day and time point); SLP, is the estimated slope related to the effect of the time-matched TAK-931 concentration $C_{TAK\text{-}931}$; and ε_{QTcF} is the residual unexplained variability of the model. Similar models were applied in the QTcP and HR analyses.

An analysis approach with an estimated correction factor was applied to derive QTcP as a sensitivity analysis to the primary analysis based on QTcF:

$$QT_cP = \frac{QT}{RR^{CF \times e^{\eta CF}}} \quad (2)$$

where CF is the estimated population typical correction factor based on pretreatment QT and RR measurements. The QTcP model described the uncorrected QT intervals under consideration of the estimated RR correction:

$$QT = (BQTcP + \eta_{BQTcP}) \times RR^{CF} + COVTIME_i + SLP \cdot C_{TAK931} + \varepsilon_{QTcF} \quad (3)$$

Apart from the estimated correction factor (RR^{CF}), the model was identical to the model of QTcF.

Covariates of interest for the concentration-ECG models were evaluated as predictors of the random baseline. The covariate evaluation was based on a stepwise "forward addition/backward elimination" covariate modeling approach based on the likelihood ratio test. Forward inclusion was performed at the $\alpha = 0.01$ significance level, corresponding to a decrease in objective function value >6.63 points for 1 degree of freedom (df = 1), whereas backward elimination was performed at the $\alpha = 0.001$ significance level (ΔOFV <10.83 points for 1 df). Backward deletion was carried out until all the remaining covariates in the model were significant at $\alpha = 0.001$.

All continuous covariates were incorporated into the population model using a scaled structure based on the median value of the covariate in the analysis data set. All categorical covariates were incorporated into the population model as a series of index variables. Coefficients of categorical covariates were estimated relative to the most prevalent category. The mathematical structures of the covariate models are shown in Table S2.

Model selection was assessed using the likelihood ratio test for hierarchical models. Standard diagnostic plots were used throughout model development to assess the ability of each model to describe observed data. The key plots included (1) observed vs population predictions and individual predictions and (2) conditional weighted residuals vs population predictions, time, time after the most recent dose, and observed TAK-931 concentration.

The resultant model from the covariate model building process evaluation was considered the final model. Overall criteria for accepting a model as final included (1) a successful minimization and covariance step, (2) no estimates close to a boundary, (3) relative standard error (RSE) <50% for covariate coefficients, and (4) no unacceptable trends in goodness-of-fit plots.

A nonparametric bootstrap analysis[15] was conducted to evaluate the stability of the final models and estimate CIs for the model parameters. The bootstrap analysis was performed with 1000 replicates of the dataset, generated by random resampling of participants from the original data set with replacement. The final model was repeatedly fitted to bootstrap replicates of the data set. CIs were calculated on the distribution of the parameter estimates from the bootstrap runs.

Visual predictive check (VPC) evaluated the predictive ability of the final model. Plots of observed data distributions were compared to corresponding simulated distributions to demonstrate the model's ability to adequately predict the data on which the model was based. VPCs were based on 500 simulations and stratified by covariates of interest.

Concentration—ECG Simulations

The final concentration-QTcF and concentration-QTcP models helped perform simulations to determine the impact of TAK-931 exposure on the respective ECG intervals in a typical patient evaluating the effect of parameter uncertainty. The effect of time described by

Table 1. Patient Demographics

Sex	
Male, n (%)	29 (60)
Female, n (%)	19 (40)
ECOG, n (%)	
0	23 (48)
1	25 (52)
Age, y, median (range)	59 (36-88)
Weight, kg, median (range)	82 (51-127)
BMI, kg/m^2, median (range)	27 (19-40)

BMI, body mass index; ECOG, Eastern Cooperative Oncology Group.

the unstructured time model was normalized by setting time to 0 hour and study day to 1.

Parameter uncertainty was implemented by replicating the simulations 500 times with parameter estimates sampled from the variance-covariance matrix of the estimate.

To assess the impact of TAK-931 exposure on ECG intervals and HR, the developed models were simulated with uncertainty to predict changes from baseline with 90%CI at the geometric mean peak plasma concentrations of TAK-931 (C_{max}) at 50 mg, a recommended phase 2 dose (RP2D) for clinical development. The model-based predictions were based on the final parameter estimates, while the 90%CIs were derived as the 5th and 95th percentile range across predictions based on 500 sets of parameter values sampled from the variance-covariance matrix of the final model estimates.

Results

Analysis Data

The analysis data set was collected from 48 participants and included 461 observations of the QTcF, QT, and HR (Table 1). The demographic profile revealed most participants were men (60%). The median participant age was 59, with a median weight of 82 kg and a median BMI of 27 kg/m^2 (Table 1). The ECOG status was approximately one-half with a 0 value and one-half with a 1 value.

Concentration—ECG Modeling Results

The initial evaluation of the Fridericia and population corrections of the observed QT intervals identified the expected strong relationship between uncorrected QT and corresponding RR intervals in the pretreatment data (Figure S1). A correction factor of 0.3962 (compared with 0.33 applied in the Fridericia correction) was estimated in the population correction, and the slopes of the relationships between QTcF and QTcP were not statistically significantly different from 0 ($P = .103$ and .993, respectively), confirming the similarity and appropriateness of both correction methods.

Linear models relating TAK-931 concentration to QTcF data acquired after oral TAK-931 administration were developed. The final model selected described a random intercept, study day, and study time as fixed factor variables; the final model also described the fixed linear effect of TAK-931 plasma concentration. QTcP

Table 2. Parameter Estimates for the Final Concentration-QTcF Model

Label	Parameter	Estimate	RSE (%)	Shrinkage (%)	Bootstrap 95%CI
BASE	THETA1	407	1	…	402 to 413
SLP	THETA3	−0.0148	42	…	−0.0273 to −0.000759
D1:H1	THETA4	2.66	67	…	−1.15 to 6.04
D1:H2	THETA5	0.922	209	…	−3.17 to 4.66
D1:H4	THETA6	3.37	48	…	0.123 to 6.57
D1:H6	THETA7	0.867	266	…	−3.84 to 5.44
D1:H8	THETA8	−3.43	54	…	−7.07 to 0.497
D3:H1	THETA9	3.45	98	…	−3.30 to 11.0
D3:H2	THETA10	1.92	153	…	−4.00 to 8.46
D3:H4	THETA11	6.02	54	…	−0.351 to 13.6
D3:H8	THETA12	−2.73	121	…	−9.09 to 4.88
D8:H1	THETA13	2.40	120	…	−3.22 to 8.19
D8:H2	THETA14	0.399	710	…	−5.26 to 6.26
D8:H4	THETA15	0.369	858	…	−6.53 to 6.63
D8:H6	THETA16	−2.76	114	…	−9.42 to 3.61
D8:H8	THETA17	−3.20	88	…	−8.67 to 2.20
D8:H24	THETA18	−1.14	246	…	−6.42 to 4.94
IIV BASE	OMEGA (1,1)	14.0	10	1	10.9 to 16.5
RUV	SIGMA (1,1)	8.95	7	5	7.45 to 9.97

BASE, estimated intercept; D, day; H, hour; IIV, interindividual variability; QTcF, Fridericia-corrected QT interval; RSE, relative standard error; RUV, residual unexplained variability; SLP, slope.

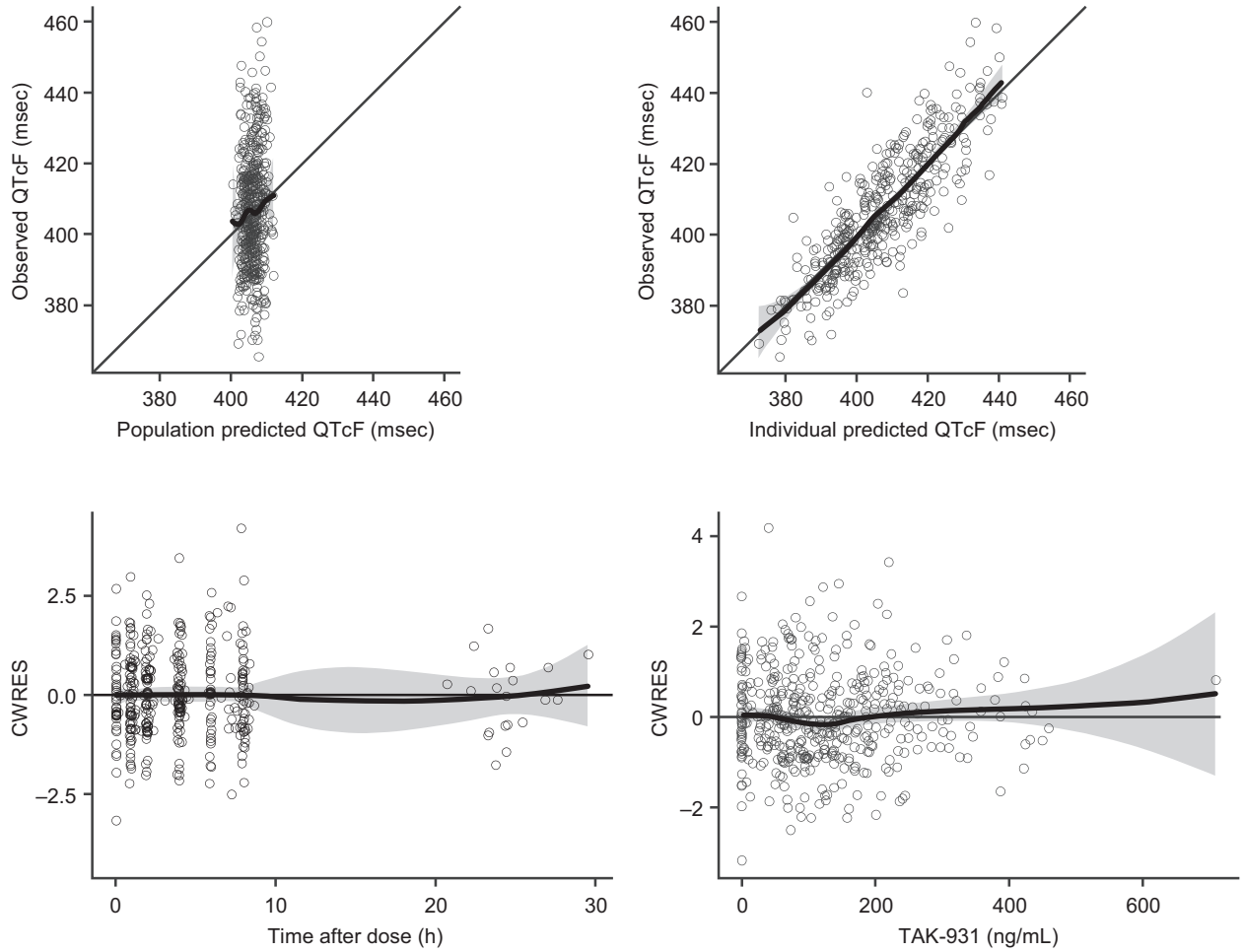

Figure 1. Goodness-of-fit and residual-based diagnostics of TAK-931 concentration-QTcF. Upper 2 panels: open circles represent individual observed versus predicted QTcF, diagonal solid black line is the line of unity. R^2 for the population-predicted and individual-predicted QTcF vs corresponding observations was 0.0119 and 0.731, respectively. Lower 2 panels: open circles are conditional weighted residuals, horizontal line is 0, gray shaded areas represent locally estimated scatterplot smoothing (LOESS) fit (95%CIs). CWRES, conditional weighted residuals; QTcF, Fridericia-corrected QT interval.

and HR were described by similar linear mixed effects models. A correction factor for RR was estimated in the QTcP model describing observed QT intervals.

Models including interoccasion variability across study days were not identifiable. Age, body weight, BMI, sex, and ECOG were evaluated as covariates on random parameters. Age was significant as a univariate covariate on the intercept in the models of QTcF ($P = .0025$) and HR ($P = .0094$) but was removed in the backward elimination ($P > .001$). As such, no statistically significant covariates were included in the final concentration-ECG models.

The parameter estimates of the final concentration-QTcF with RSE, shrinkage, and the bootstrap 95%CIs are shown in Table 2; similar data for HR are shown in Table S3. Goodness-of-fit plots and residual-based diagnostics suggested that the model was adequate for predicting mean changes in QTcF (Figure 1) and HR (Figure 2). VPC confirmed that the model for QTcF (Figure 3A and B) and HR (Figure 3C and D) adequately described the median and 5th and 95th percentile of the observed data across time since last dose (Figure 3A and C) and observed TAK-931 plasma concentration (Figure 3B and D). The goodness-of-fit plots are shown for QTcP (Figure S2). Parameter estimate is also presented for HR (Table S3) and QTcP (Table S4). VPC data are presented for QTcP (Figure S3).

The model-based prediction of QTcF change from baseline vs TAK-931 plasma concentration is shown in Figure 4A; similar data for HR are presented in Figure 4B. Additional graphical representations of the predictions of the models are presented in the supplemental figures for QTcP (Figure S4). Predictions were computed for the steady-state geometric mean C_{max} of 231 and 341 ng/mL achieved after administration of

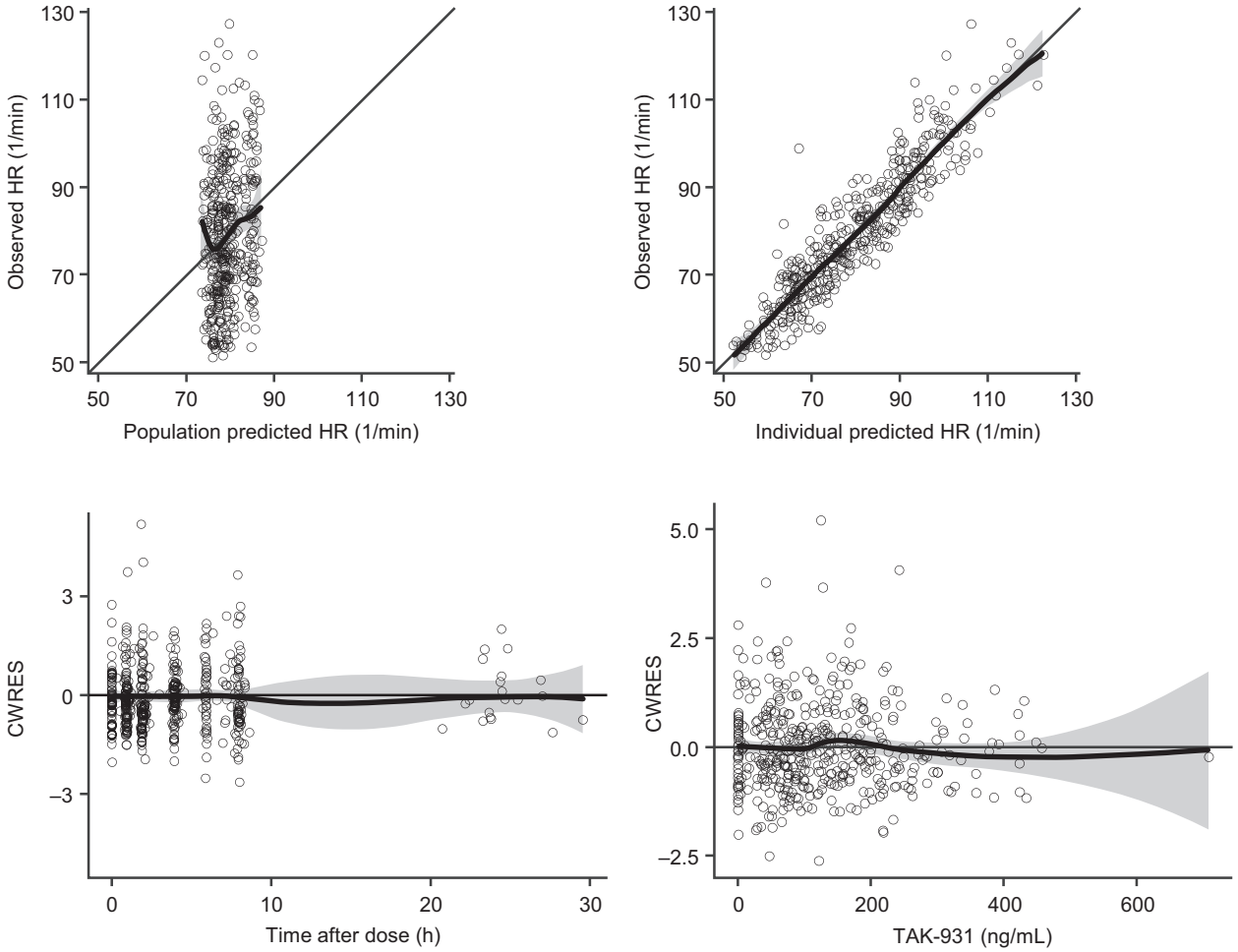

Figure 2. Goodness-of-fit and residual-based diagnostics of TAK-931 concentration-HR. Upper 2 panels: open circles represent individual observed versus predicted HR, diagonal solid black line is the line of unity. R^2 for the population-predicted and individual-predicted HR versus corresponding observations was 0.0282 and 0.859, respectively. Lower 2 panels: open circles are conditional weighted residuals, horizontal line is 0, gray shaded areas represent locally estimated scatterplot smoothing (LOESS) fit (95%CI). CWRES, conditional weighted residuals; HR, heart rate.

TAK-931 at 50 and 80 mg once daily, respectively, for 14 days in a 21-day cycle.

A change in QTcF of −3.41 milliseconds (90%CI, −5.77 to −1.17 milliseconds) was predicted at the geometric mean C_{max} of 231 ng/mL. For a C_{max} of 341 ng/mL, the change in QTcF was −5.03 (90%CI, −8.52 to −1.73). The QTcP model predicted a change of −2.02 milliseconds (90%CI, −4.15 to 0.0679 milliseconds) at the same concentration. For a C_{max} of 341 ng/mL, the change in QTcP was −2.99 (90%CI, −6.13 to 0.100).

An HR change of 3.40 min^{-1} (90%CI, 1.86-4.80 min^{-1}) was predicted at TAK-931 plasma concentration of 231 ng/mL, the geometric mean C_{max} after TAK-931 oral dose at 50 mg. At 341 ng/mL, an HR change of 5.01 min^{-1} (90%CI, 2.74-7.08 min^{-1}) was predicted. A noticeable delay between TAK-931 concentration and HR response was present. However, this delay was corrected by the unstructured model of time. Model-predicted ECG intervals and HR at the geometric mean of TAK-931 C_{max} after oral administration at 50 and 80 mg are shown in Table 3.

Discussion

The effect of TAK-931, an investigational, orally administered small-molecule cell division cycle 7 inhibitor, on QTc intervals was evaluated in 48 patients with advanced solid tumors in 2 clinical trials. TAK-931 is a cytotoxic agent and cannot be administered at supratherapeutic doses or repeated exposures to healthy volunteers. Accordingly, a placebo or positive control (eg, moxifloxacin) was not included in the assessment, which is consistent with approaches used in evaluating effects of anti-cancer agents on QTc.[16] The data from the 2 studies in which patients were treated

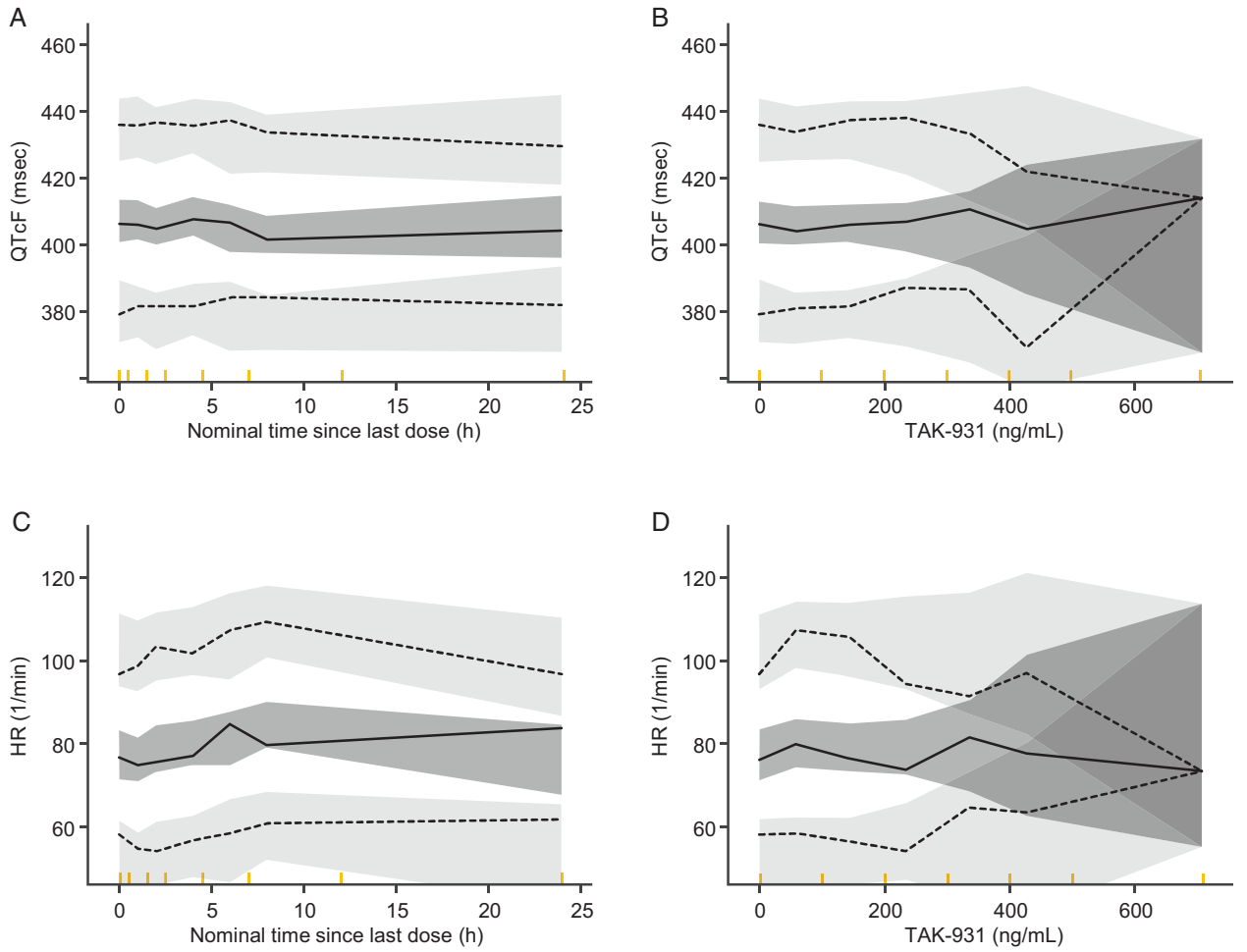

Figure 3. Visual predictive check of TAK-931 concentration-QTcF model (A, B) and TAK-931 concentration-HR model (C, D) showing observed data and model predictions across time since last dose (A, C) and observed TAK-931 plasma concentration (B, D). Solid and dashed black lines show the median and 5th and 95th percentiles of the observed data in bins indicated by yellow pins across time since last dose and observed plasma TAK-931 plasma concentration. Dark and light shaded areas show 95%CI of corresponding model predictions. HR, heart rate; QTcF, Fridericia-corrected QT interval.

with TAK-931 at 2 doses (50 and 80 mg) consisted of PK time-matched, centrally read, triplicate ECG that allowed population-based models to examine the relationships between ΔQTcF, ΔQTcP, HR vs TAK-931 plasma concentrations. Approximately 13.4% (62/461) of data records had higher concentration values than the geometric mean C_{max} of the 50-mg daily dose (231 ng/mL), which is an RP2D for clinical development. As such, the data from the 2 clinical trials were considered to not only provide QT assessment at TAK-931 plasma concentrations in the therapeutic range but also in the supratherapeutic range. There was no clinically relevant effect of TAK-931 on the QT intervals after dosing at 50 mg once daily in a 21-day cycle, the RP2D in clinical development, as supported by the model estimated upper bound of the 90%CIs of ΔQTcF and ΔQTcP. This value was well below 5 milliseconds at the geometric mean C_{max} at 50-mg once-daily dosing. TAK-931 concentrations were correlated with an increase in HR. Hysteresis plots indicated a delay between increasing TAK-931 concentrations and the subsequent increases in HR. These effects were accounted for by the unstructured time component in the direct linear effect model.

The cardiac effects of TAK-931 exposure were represented by a linear slope describing the relationship between TAK-931 plasma concentration and the observed ECG intervals and HR. A statistically significant slope could only be identified in the models of QTcF intervals and HR. QTcF was predicted to decrease by 0.0148 milliseconds per ng/mL increase in plasma TAK-931 concentration. The RSE on this estimate was 42% and the corresponding 90%CI was −0.0273 to −0.000759, indicating only a marginally significant effect. The HR model predicted the effect of TAK-931 to be a 0.0147 beats-per-minute increase per ng/mL in plasma TAK-931 concentration. The associated RSE

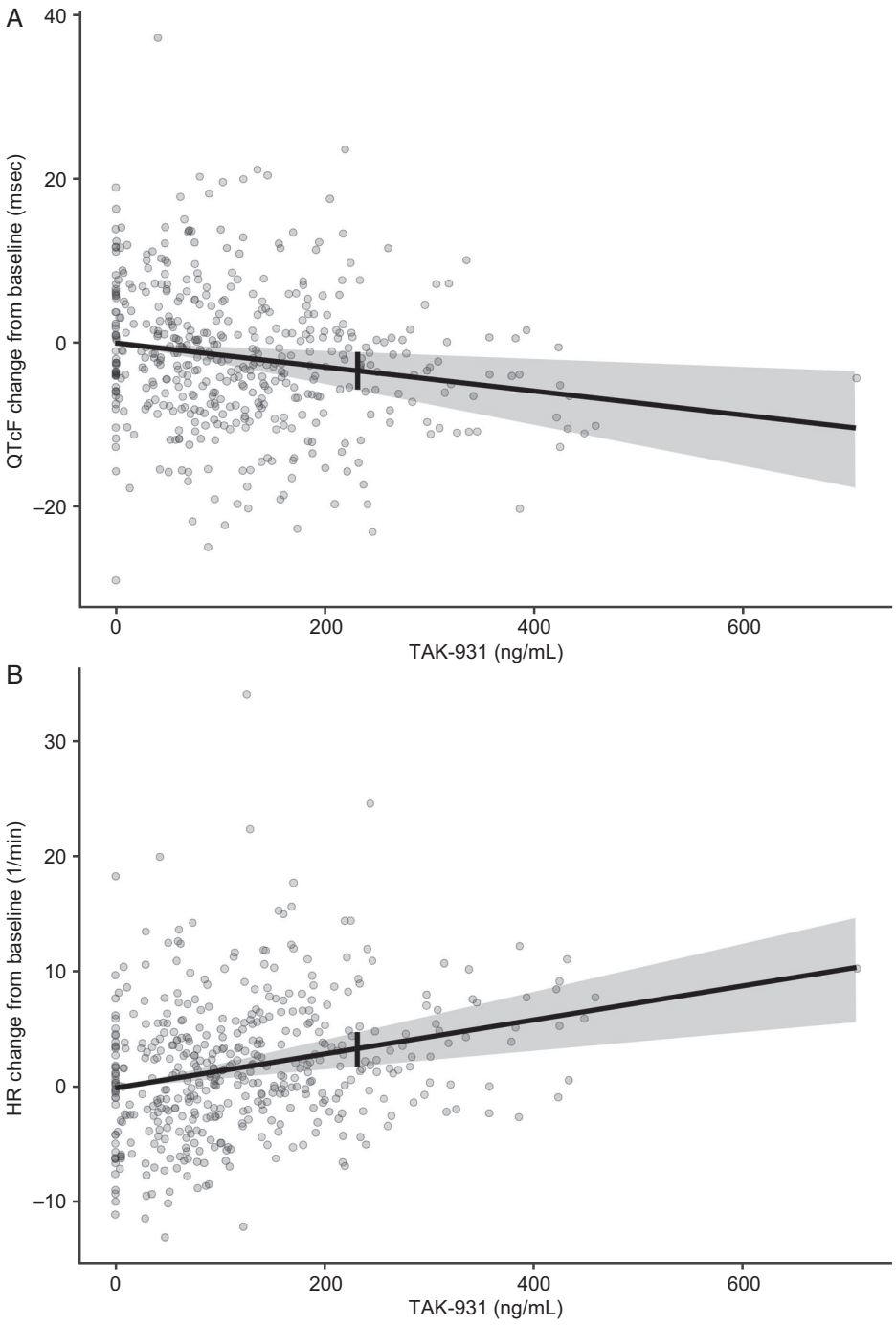

Figure 4. Model-predicted QTcF (A) and HR (B) change from baseline vs TAK-931 plasma concentration based on the concentration-QTcF and concentration-HR models, respectively. Black line (gray area) shows the model prediction (90%CI). Vertical black line segments indicate the estimated change of QTcF (A) and HR (B) and associated 90%CI at the geometric mean of C_{max} following administration of 50 mg TAK-931 QD (231 ng/mL). HR, heart rate; QTcF, Fridericia-corrected QT interval.

and 90%CI were 26% and 0.00629-0.0226 beats per minute/(ng/mL). The population-corrected QT model did not identify statistically significant relationships between TAK-931 concentration and these intervals.

In conclusion, the current model-based analysis indicated a lack of clinically meaningful effects of TAK-931 on the electrocardiographic QTc interval. The integrated analysis of triplicate, centrally read ECG, and time-matched PK data collected from early clinical studies provided an alternative approach in lieu of a dedicated study to assess the effects of new anticancer candidates on QT intervals.

Table 3. Model-Based Simulations of Baseline-Corrected ECG Intervals and HR at the Geometric Mean C_{max} After 50 mg Dose

ECG Interval/HR	C_{max} (ng/mL)	Model Prediction (90%CI)
ΔQTcF (millisecond)	231	−3.41 (−5.77 to −1.17)
QTcP (millisecond)	231	−2.02 (−4.15 to 0.0679)
ΔHR (beats per minute)	231	3.40 (1.86 to 4.80)

C_{max}, maximum concentration; ECG, electrocardiogram; HR, heart rate; ΔQT, representation of QTcP model prediction; QTcF, Fridericia-corrected QT interval; QTcP, population-corrected QT interval.

Acknowledgments

The authors thank all patients included in this analysis and their families, as well as all physicians, nurses, study coordinators, and study center staff participating in these 2 studies. The authors also thank eRT (Philadelphia, Pennsylvania) for the central reading of the triplicate ECGs. The authors were assisted in the preparation of the manuscript by Robert Lersch of Lersch Global Communications, LLC under the supervision of the authors. This assistance was funded by Takeda Development Center Americas, Inc.

Conflicts of Interest

N.G. and X.Z. are current employees of Takeda Development Center Americas, Inc. P.M.D. is an employee of Certara, Data Science Services, which was compensated by Takeda for the analyses performed.

References

1. Kurasawa O, Miyazaki T, Homma M, et al. Discovery of a novel, highly potent, and selective thieno[3,2-d]pyrimidinone-based Cdc7 inhibitor with a quinuclidine moiety (TAK-931) as an orally active investigational antitumor agent. *J Med Chem*. 2020;63(3):1084-1104.
2. Iwai K, Nambu T, Dairiki R, et al. Molecular mechanism and potential target indication of TAK-931, a novel CDC7-selective inhibitor. *Sci Adv*. 2019;5(5):eaav3660.
3. Zhou X, Ouerdani A, Diderichsen PM, Gupta N. Population pharmacokinetics of TAK-931, a cell division cycle 7 kinase inhibitor, in patients with advanced solid tumors. *J Clin Pharmacol*. 2022;62:422-433.
4. Millennium Pharmaceuticals Inc, Takeda. A study to evaluate TAK-931 in participants with advanced nonhematologic tumors. https://ClinicalTrials.gov/show/NCT02699749. Published December 21, 2019. Accessed April 7, 2021.
5. Millennium Pharmaceuticals Inc, Takeda. A study to evaluate the safety, tolerability, and activity of TAK-931 in participants with metastatic pancreatic cancer, metastatic colorectal cancer, and other advanced solid tumors. https://ClinicalTrials.gov/show/NCT03261947. Published August 24, 2020. Accessed April 7, 2021.
6. Millennium Pharmaceuticals Inc, Takeda. A study to assess the relative bioavailability, effect of food, and gastric potential hydrogen (pH) modification on the pharmacokinetics (PK) of TAK-931 in participants with advanced solid tumors. https://ClinicalTrials.gov/show/NCT03708211. Published December 3, 2019. Accessed April 7, 2021.
7. Garnett CE, Zhu H, Malik M, et al. Methodologies to characterize the QT/corrected QT interval in the presence of drug-induced heart rate changes or other autonomic effects. *Am Heart J*. 2012;163(6):912-930.
8. Lester RM. Update on ICH E14/S7B cardiac safety regulations: the expanded role of preclinical assays and the "double-negative" scenario. *Clin Pharmacol Drug Dev*. 2021;10(9):964-973.
9. Garnett C, Bonate PL, Dang Q, et al. Scientific white paper on concentration-QTc modeling. *J Pharmacokinet Pharmacodyn*. 2018;45(3):383-397.
10. Faucette S, Wagh S, Trivedi A, Venkatakrishnan K, Gupta N. Reverse translation of US Food and Drug Administration reviews of oncology new molecular entities approved in 2011-2017: lessons learned for anticancer drug development. *Clin Transl Sci*. 2018;11(2):123-146.
11. Zhou X, Nemunaitis J, Pant S, et al. Effect of alisertib, an investigational aurora a kinase inhibitor on the QTc interval in patients with advanced malignancies. *Invest New Drugs*. 2018;36(2):240-247.
12. Gupta N, Huh Y, Hutmacher MM, Ottinger S, Hui AM, Venkatakrishnan K. Integrated nonclinical and clinical risk assessment of the investigational proteasome inhibitor ixazomib on the QTc interval in cancer patients. *Cancer Chemother Pharmacol*. 2015;76(3):507-516.
13. Dixon JR, Jr. The International Conference on Harmonization Good Clinical Practice guideline. *Qual Assur*. 1998;6(2):65-74.
14. Widerlöv E, Jostell KG, Claesson L, Odlind B, Keisu M, Freyschuss U. Influence of food intake on electrocardiograms of healthy male volunteers. *Eur J Clin Pharmacol*. 1999;55(9):619-624.
15. Yafune A, Ishiguro M. Bootstrap approach for constructing confidence intervals for population

pharmacokinetic parameters. I: a use of bootstrap standard error. *Stat Med*. 1999;18(5):581-599.
16. Rock EP, Finkle J, Fingert HJ, et al. Assessing proarrhythmic potential of drugs when optimal studies are infeasible. *Am Heart J*. 2009;157(5):827-836, 836 e821.

Supplemental Information

Additional supplemental information can be found by clicking the Supplements link in the PDF toolbar or the Supplemental Information section at the end of web-based version of this article.